Cerium Dioxide Nanoparticles Induce Apoptosis and Autophagy in Human Peripheral Blood Monocytes

Salik Hussain[†,*], **Faris Al-Nsour**[†], **Annette B. Rice**[†], **Jamie Marshburn**[†], **Brenda Yingling**[†], **Zhaoxia Ji**[‡], **Jeffrey I. Zink**[‡], **Nigel J. Walker**[§], and **Stavros Garantziotis**[†]

[†]Clinical research unit, National Institute of Environmental Health Sciences, (NIEHS)/National Institute of Health (NIH), Research Triangle Park 27709, NC, USA

[‡]UC Center for Environmental Implications of Nanotechnology University of California, Los Angeles, CA

[§]Division of the National Toxicology Program (NTP), National Institute of Environmental Health Sciences (NIEHS)/National Institute of Health (NIH), Research Triangle Park 27709, NC, USA

Abstract

Cerium dioxide nanoparticles (CeO_2 NPs) have diversified industrial uses and novel therapeutic applications are actively being pursued. There is lack of mechanistic data concerning the effects of CeO_2 NPs on primary human cells. We aimed at characterizing the cytotoxic effects of CeO_2 NPs in human peripheral blood monocytes. CeO_2 NPs and their suspensions were thoroughly characterized, including using transmission electron microscopy (TEM), dynamic light scattering (DLS), and zeta potential analysis. Blood from healthy human volunteers was drawn through phlebotomy and CD14+ cells were isolated. Cells were exposed to CeO_2 NPs (0.5–10 μg/mL) for 20 or 40 hours and mechanisms of cell injury were studied. TEM revealed that CeO_2 NPs are internalized by monocytes and are found either in vesicles or free in the cytoplasm. CeO_2 NP exposure leads to decrease in cell viability and treated cells exhibit characteristic hallmarks of apoptosis (activation of Bax, loss of mitochondrial membrane potential, DNA fragmentation). CeO_2 NP toxicity is caused by mitochondrial damage leading to apoptosis inducing factor (AIF) release, but not due to caspase activation or reactive oxygen species production. Moreover, CeO_2 NP exposure leads to autophagy, which is further increased after pharmacological inhibition of

[*]Corresponding Author: Salik Hussain DVM, PhD, Clinical Research Unit, National Institute of Environmental Health Sciences, Research Triangle Park, 27709, Durham, NC., Tel: +1 919 316 4806, Fax: +1 919 541 9854, salik.hussain@nih.gov.

Conflict of Interest: None

Supporting Information Available:
Supplementary Experimental Details
Supplementary Table S1. Population demographics
Supplementary FigureS1. DLS analysis of CeO_2 NPs
Supplementary Figure S2. TEM images of CeO_2 NP suspension and NP aggregate in vesicle inside a human monocyte
Supplementary Figure S3. ROS production in CeO_2 NP treated cells
Supplementary Figure S4. Role of ROS production in cell injury response to CeO_2 NPs
Supplementary Figure S5. Evaluation of caspase activation in cell death response to CeO_2 NPs
Supplementary Figure S6. Role of chemical nature in the induction of biological responses; comparison of CeO_2 with carbon black
Supplementary Figure S7. Evaluation of the role of surface coating of nutrients/corona on the toxicity of CeO_2 NPs.
This material is available free of charge *via* the Internet at http://pubs.acs.org.

tumour suppressor protein p53. Inhibition of autophagy partially reverses cell death by CeO_2 NPs. It is concluded that CeO_2 NPs are toxic to primary human monocytes at relatively low doses.
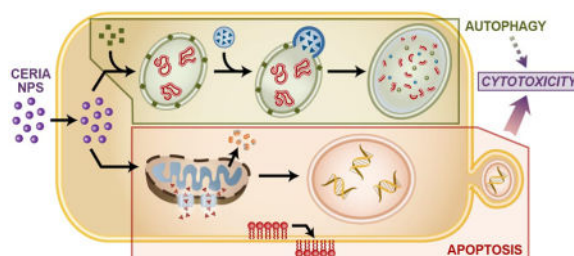
Keywords

Cerium dioxide/ceria; nanoparticle; toxicity; apoptosis; autophagy; monocytes; ultrafine

Nanoparticle-size cerium dioxide (CeO_2 NPs) has gained increased attention in the recent past, due to its diverse uses. In industrial settings CeO_2 NPs are used in catalysis, ultraviolet absorbance, oxygen sensing, solar and fuel cells and polishing (for glasses, lenses, television tubes, fuel cell and precision optics). [1–5] In addition to these industrial applications, CeO_2 NP use in therapeutics has also been proposed, such as in antioxidant therapy, neuroprotection, radioprotection and ocular protection. [6–10] Furthermore, CeO_2 NPs are of significant environmental health interest, since CeO_2 NPs containing diesel fuel additives are used in many countries to reduce the emission of particulate matter (PM) from diesel engines. [11] However, the human health effects of the resultant increased emission of CeO_2 NPs are unknown. According to the Health Effects Institute (HEI) CeO_2 NPs emissions were expected to reach up to 22 million pounds annually in the European Union after introduction of diesel-additive nano CeO_2. [12] Importantly, most of the CeO_2 released as a result of combustion is in the form of NPs. [13] For all these reasons, the Organization for Economic Cooperation and Development (OECD) has included CeO_2 NPs in the priority list of the nanomaterials requiring urgent evaluation. [14]

Health effects of NPs in general and CeO_2 NPs in particular are still a matter of continued debate. *In vitro* and *in vivo* experiments suggest that CeO_2 NPs produce reactive oxygen species (ROS), inflammation, lipid peroxidation, lung damage and altered macrophage phenotypes. [15–16] Furthermore, CeO_2 NPs have acute and chronic fibrotic and inflammatory effects in murine lungs. [17] However, there are also reports of CeO_2 NPs acting as antioxidant and as an anti-inflammatory agent. [18–19] Variability in examined target species and cell type, experimental setup (exposure concentration and duration) and NPs used- (shape, size, purity and surface modifications) complicate the accurate assessment of CeO_2 NPs effects.

It is now known that different modalities of cell death (apoptosis, necrosis, autophagy) contribute to the pathophysiology of different human disorders (cancer, neurodegenerative diseases, sepsis etc). [20–22] Moreover, it has been shown that autophagy (generally thought to be a survival mechanism) is also a programmed cell death process besides apoptosis. [23] A better understanding of the interaction of NPs with these pathways of cell injury can help in

developing the counter strategies for different human disorders as well as well as will help in formulation of safe and consumer friendly nanotechnology. Keeping in view the proposed nanomedical applications of CeO_2 NPs, an evaluation of such interactions become even more pertinent as these could result in potential unwanted consequences.

Most studies addressing potential toxic effects of CeO_2 NPs were performed either in immortalized cell lines, or non-human cells. Furthermore, doses used in some of the studies far exceed what is likely to be a relevant range for human environmental or pharmacological exposure. We therefore studied effects of low-dose (nM-μM) CeO_2 NPs in human primary monocytes. We demonstrate that CeO_2 NP exposure leads to the cytotoxicity in monocytes associated with an induction of mitochondria-mediated apoptosis and autophagy. To the best of our knowledge this is the first report on the effects of CeO_2 NPs in primary human cells in general and in human peripheral blood monocytes in particular.

Results

NP characterization

Detailed physicochemical characteristics of CeO_2 NPs in dry state and after suspending in cell culture medium or water are presented in Table1 and Supplementary Figure S1. In the environment CeO_2 will exist likely as both dispersed and aggregated forms. Respirable "particle" size is <3um so NP sizes and aggregated are relevant for human exposures. TEM images of NPs are shown in Supplementary Figure S2 showing the irregular shape and aggregation of CeO_2 NPs.

CeO_2 NPs induce ultrastructural alterations

TEM analysis revealed that CeO_2 NPs are incorporated by CD14+ cells (Figure 1). CeO_2 NPs were found inside cells as electron dense material either free in cytoplasm or as membrane bound aggregates. Pathological changes included an increase in phagolysosomes, increase in Golgi (with minimal dilated cisterns), increased formation of autophagic vesicles and a mild increase in mitochondrial swelling together with mitochondrial elongation. Phagolysosomes had CeO_2 NPs, cellular debris, myelin figures, membrane fragments, and occasionally, small lipid droplets. Most cells, showed diffuse cytoplasmic expansion after exposure to CeO_2 NPs.

CeO_2 NPs induce apoptosis

After 40 hours exposure to 5 and 10 μg/mL CeO_2 NPs a significant decrease in viability of monocytes was observed (Figure 2A). Further evaluation of the mode of cell death revealed that this loss of viability was mainly due to apoptosis (Figure 2B). Moreover, we observed significant DNA fragmentation after exposure to CeO_2 NPs (Figure 2C).

CeO_2 NPs induce mitochondrial damage

A significant number of cells (20–25%) with activated form of a pro apoptotic protein Bax (relocated to the mitochondria) were observed following 5 and 10 μg/mL CeO_2 NPs exposure for 40 hours (Figure 3A, 3B). An increase in mitochondrial depolarization (loss of mitochondrial membrane potential;$\downarrow \psi_m$)) was also observed after CeO_2 NPs exposures

(Figure 3C). It is noteworthy that we did not observed activation of caspase-3/-7 after exposure to CeO_2 NPs and pre-treatment with pan caspase inhibitor (Z-Vad Fmk) did not protect from apoptosis (Supplementary Figure S3). However, an increase in the protein levels of Apoptosis Inducing Factor (AIF), known to induce caspase-independent apoptosis and DNA fragmentation), was observed after NP exposures (Figure 3D). A mild ROS production response was noted after exposure to CeO_2 NPs (Supplementary Figure S4). This ROS appeared to be mainly comprised of superoxide anions ($O_2^{\bullet-}$) produced due to mitochondrial damage (Supplementary Figure S5). However, successful inhibition of $O_2^{\bullet-}$ production using PEG-catalase failed to rescue cells from undergoing apoptosis (Supplementary Figure S5).

CeO_2 NPs induce autophagy

CeO_2 NPs exposure led to significant increase in lysotracker red uptake (Figure 4A) and increased number of LC3b+ vesicles (Figure 4B, 4C). These results were further confirmed by detection of monodansylcadaverine (MDC) positive autophagic vacuoles (data not shown).

p53 inhibition amplifies CeO_2 NPs-induced autophagy

As p53 can differentially regulate both apoptosis and autophagy, we further explored whether p53 inhibition (using the pharmacological inhibitor pifithrin-α (PFT-α)) can modulate CeO_2 NP induced apoptosis and autophagy (Figure 5). We observed that p53 inhibition has no effect on CeO_2 NP-induced apoptosis (Figure 5A, 5B) however it leads to increase in the autophagy (Figure 5C).

Crosstalk between CeO_2 NPs induced autophagy and apoptosis

Wortmannin (an autophagy inhibitor) treatment completely inhibited the autophagy induced by CeO_2 NPs (Figure 6A) and led to a 30–58% increase in the viability of CeO_2 NP treated cells (Figure 6B). This increase in viability was partly (20–35%) due to decrease in the apoptosis induced by CeO_2 NPs (Figure 6C). These results suggest that autophagy contribute to the cell injury response induced by CeO_2 NPs.

Discussion

This experimentation aimed at deciphering the effects of CeO_2 NPs on human monocytes. We demonstrate a significant toxic response after 20–40 hours exposure to CeO_2 NPs which involved the induction of type 1 and type 2 programmed cell death processes (apoptosis and autophagy). CeO_2 NP induced apoptosis involved mitochondrial damage and AIF expression. In addition, CeO_2 NP induced autophagy contributed to the cytotoxicity and was found to be modulated by p53.

We demonstrate here that CeO_2 NP exposure leads to induction of autophagy in a time-and dose-dependent manner in human monocytes. Indeed, exposure to different types of NPs (*e.g.* fullerenes, quantum dots, rare earth metals) has been shown to induce autophagic events in cultured cells. [24–26] The exact mechanism how CeO_2 NPs induce autophagy is unclear, and could involve the direct interaction with endosomes/lysosomes themselves

(since CeO_2 NPs appear to accumulate in these compartments), overexpression of genes for vesicle formation, or identification of NPs as foreign endosomal pathogen. Moreover, an association of p53 with either apoptosis or autophagy or even both processes has been recently demonstrated. [27] We therefore explored the role of p53 in CeO_2 NP induced cell death pathways. Interestingly we found that apoptosis induction after CeO_2 NPs exposure is independent of p53 involvement. However a significant increase in autophagy after p53 inhibition was observed. Indeed, Tasdemir *et al* have recently shown the negative regulation of autophagy by cytoplasmic p53. [28] They demonstrated that depletion or pharmacologic inhibition of cytoplasmic p53 in cell lines and in mice induces autophagy. We show for the first time that in the case of existing autophagic events such p53 inhibition can lead to an increase in autophagy. This could be due to the direct interaction of CeO_2 NPs with cytoplasmic p53. It has been postulated that many of the observed adverse effects of NPs are due to their interaction with proteins, leading to change in protein conformation and irreversible loss of activity (in case of enzymes). [29–30] Further experimentation is needed to understand this process in the case of CeO_2 NPs.

The fact that induction of autophagy was mainly observed at the doses causing cytotoxicity, suggests that upregulation of autophagy is part of the cytotoxic response. It is now known that autophagy can promote cell death by selectively removing survival factors and prolonged removal of cellular constituents resulting in the demise of cells. [31] In our study the role of autophagy as a contributor to the cell death is further confirmed by the fact that pre-treatment with the autophagy inhibitor wortmannin causes up to 50% reduction in cell death.

An interesting ultra-structural finding was the swelling and elongation of mitochondria in CeO_2 NP treated cells. Recently, it has been shown that mitochondrial elongation can also occur due to unopposed mitochondrial fusion during autophagy process and is an attempt to maintain cell viability. [32] These elongated mitochondria can avoid trapping in the autophagic vesicles due to steric hindrance. It is also known that mitochondrial structural and functional changes play an important role in wide variety of different cellular processes, including apoptosis. [33] We demonstrate mitochondrial damage in human monocytes after CeO_2 NP exposure leading to the induction of apoptosis. We observed activation and relocation of Bax to the mitochondria and decrease in mitochondrial membrane potential ($\downarrow \psi_m$) after exposure to CeO_2 NP. This $\downarrow \psi_m$ is an early event for the apoptosis process as it was observed at early time points, while no cell death was evident. Furthermore, apoptosis appeared to be caspase-independent (no activation of caspase 3 or 7 and no protection by pan-caspase inhibitor (Zvad-FMK) (Supplementary Figures S3). However, we observed increased protein expression of AIF which has already been shown to induce caspase-independent apoptosis and DNA fragmentation. [34] Moreover, we show that $O_2^{\bullet-}$ production occurs as a result of mitochondrial damage and does not contribute to cell death induction, since their inhibition does not protect from CeO_2 NP-induced cytotoxicity (Supplementary Figure S4 and S5).

A summary of the mechanisms that we have demonstrated to be involved in CeO_2 NP induced toxicity is presented in Figure 7. The toxic response to CeO_2 NP exposure is mediated both by autophagy and mitochondrial-mediated apoptosis. Autophagy contributes

to cytotoxicity both directly and indirectly, *via* induction of apoptosis. However, mitochondrial damage appears to be the primary mechanism as autophagy inhibition leads only to approximately 35% reduction in apoptosis induction. These responses seem to be specific to CeO_2 NPs sine they did not occur after carbon black NP exposure at similar concentrations and durations (Supplementary Figure S6) and were not a consequence of adsorption of nutrients on the surface of the particles (Supplementary Figure S7).

Our results have significant implications. Human monocytes are an integral part of immunity. Monocytes can initiate or amplify an inflammatory response and are precursors of dendritic cells and tissue macrophages. Moreover, they link the innate immunity to adaptive immune responses. Thus monocyte apoptosis by NPs can lead to lowered ability to mount an effective immune response early after infection, as has been demonstrated for other engineered NPs, particulate matter and other pollutants [35–37] Furthermore, recently it has been shown that autophagy in antigen presenting cells can lead to the initiation and/or progression of autoimmune processes. [38] Further *in vivo* studies are currently underway in our laboratory to establish the biological relevance of CeO_2 NP induced monocyte apoptosis *in vivo*.

Conclusion

In summary this study provides potential mechanistic pathways for CeO_2 NP-induced cell injury. We demonstrate that CeO_2 NPs induce cytotoxicity through autophagy and mitochondrial apoptosis pathway in *ex-vivo* cultured human peripheral blood monocytes. Further *in vivo* studies are warranted to elaborate the consequences of CeO_2 NPs induced autophagy and apoptosis. Our results however underscore the urgent need for the rational toxicological assessment of novel nanomaterials at relevant exposure levels. Moreover, for realistic hazard identification of nanomaterials the preferred *in vitro* system should include primary human cells.

Methods

Nanoparticles

CeO_2 NPs were acquired from Meliorum Technologies (Rochester, NY) and characterized by University of California, Center for Environmental Implications of Nanotechnology (CEIN). NPs were characterized for shape/diameter (transmission electron microscopy (TEM), crystal structure (X-ray diffraction analysis-XRD), surface area (Brunauer-Emmitt-Teller method, BET), suspension behaviours-hydrodynamic diameter and size distribution (dynamic light scattering-DLS), Zeta potential (ζ potentials) (Malvern Zeta sizer), purity (thermogravimetric analysis-TGA) and bacterial endotoxins (limulus amebocyte lysate assay). TGA analysis revealed that CeO_2 NPs were 95.14% (wt%) pure and contained 4.1% moisture and 0.85% acid contents. NP stock solution (1mg/mL) was prepared in water and stored at 4°C in a refrigerator. All exposure suspensions were freshly prepared from this stock solution after sonication (3 pulses of 20 seconds at 235W each with 5 second pause using Mesonix S 4000 cuphorn sonicator (Qsonica LLC, Newtown, CT). After sonication the particles were suspended in cell culture medium and used to expose cells within 5 minutes after vortexing.

Dynamic light scattering (DLS) analysis of CeO_2 NPs suspensions (at the highest utilized concentration; 10 μg/mL) in cell culture medium was done to analyze size distribution and measure zeta potentials of NPs using ZetaSizer Nano (Malvern Instruments, Westborough, MA). Electrophoretic mobility (an approximation of particle surface charge) was converted into zeta potential using the Helmholtz-Smoluchowski equation.

Study Subjects and isolation of cells

This study was approved by the NIEHS Institutional Review Board. Adult human volunteers without history of chronic medical conditions or chronic medication use were recruited to the NIEHS Clinical Research Unit. Population demographics are presented in Supplementary Table S1. Whole blood was withdrawn from an antecubital vein into citrated tubes. Mononuclear fraction was isolated by gradient centrifugation using histopaque (Sigma Aldrich, St. Louis, MO). Cells were labeled with CD14 magnetic beads and positively selected using magnetic column according to manufacturer recommendations (Miltenyi Biotec, Boston, MA). By this method 95–99% viable pure human monocytes were obtained, confirmed by flow cytometery and cytospin preparations.

Cells and Culture Conditions

After isolation, cells were seeded in 24 well cell culture plates (400,000 cells per well) in *Ex-Vivo* cell culture medium (Lonza) supplemented with 1% human serum and antibiotics [1% solution of penicillin (100μg/mL) and streptomycin(100μg/mL), Invitrogen Carlsbad, CA] and incubated at 37°C, 5% CO_2 and 95% relative humidity for 2 hours. Cell culture medium was then aspirated and cells were washed thoroughly with fresh medium to remove unattached cells. Cells were then incubated in fresh pre-warmed medium containing desired doses of NPs for different time points (20 or 40 hours). Although a direct dose comparison between *in vivo* and *in vitro* studies is challenging, we chose CeO_2 NP doses that represent the lower end of what is reported in the literature. [16, 19, 39–40] Furthermore, the doses used for our assays (0.5–10 μg/ml i.e 2.9–58 μM) lie in the possible long term human exposure range, because CeO_2 is cleared from human lungs over a period of many years. [41]

In experiments requiring pre-treatment with inhibitors, cells were first incubated with inhibitor containing *ex-vivo* medium as described below and then exposed to fresh NPs suspensions in medium containing inhibitors. At the end of treatment period cells were trypsinated using 0.025% trypsin-EDTA (Invitrogen). Action of trypsin was inhibited using 10% fetal bovine serum (Sigma Aldrich, St. Louis, MO). In some experiments, Polyethylene glycol coated catalase (PEG-catalase, Sigma Aldrich, St. Louis, MO) pre-treatment was done for 30 minutes (1000 IU) and then cells were treated with CeO_2 NPs. Similar protocol with 2 hours pre-incubation was followed for p53 inhibitor (pifithrin-alpha) and autophagy inhibitor wortmannin (both from Sigma Aldrich).

TEM analysis of NP-cell interaction

Human peripheral blood monocytes were grown in 2 chamber cell culture slides and treated with different concentrations of CeO_2 NPs for 40 hours. The cells were fixed in 3% gluteraldehyde, thin sections (60–90 nm) were cut and placed on formvar copper grids then

stained with uranyl acetate and lead citrate. After staining sections were examined on a FEI Tecnai 110KV microscope at 80KV and digital photomicrographs were taken.

Cell Viability analysis

Cells were seeded in 96 well plates (at 50,000 cells/well density) and treated with different concentrations (0.5–10 μg/mL) of CeO_2 NPs for 20 or 40 hours. Cells were then incubated with 10 μM Calcein-AM (Invitrogen) for 1 hour. The green fluorescence from viable cells (produced due to esterase activity in the living cells) was analyzed at 485nm excitation and 530 nm emission wavelengths. NP-treated cells without Calcein-AM and Calcein-AM alone with NPs (without cells) was also analyzed to rule out possible interferences with the assay. The results are presented as percent of control.

DNA fragmentation (Sub-G1 peak) analysis

Sub-G1 peak analysis was performed according to the method described previously. [42] Cells were analysed using BD Facsort flow cytometer for 535 nm excitation and 617 nm emission wavelengths for PI. At least 7500 cells were analysed to determine the percentage of cells in the Sub-G1 region.

Annexin-V/Propidium Iodide (PI) staining

Annexin-V/PI labelling was performed according to manufacturer's recommendations (Invitrogen). Analysis was performed on BD FACSAria II instrument. At least 10000 cells were analysed to determine the percentage of apoptotic cells. The results are presented as percentage of apoptotic cells (early + late apoptotic cells). However, it is noteworthy that majority of the positive cells (>90%) were early apoptotic cells.

Mitochondrial membrane potential (ψ_m) Changes

Changes in ψ_m were monitored after staining with JC-1 probe (Invitrogen) as described elsewhere. [43] Analysis was performed on BD FACSAria II instrument.

Immunocytochemistry

Staining for activated Bax and microtubule-associated protein 1 light chain 3 (LC3B) was performed on paraformaldehyde (4%) fixed cells as described previously. [44] Mouse anti Bax (6A7, Sigma Aldrich) and rabbit recombinant oligoclonal antibody (Invitrogen) were used as primary antibodies and Alexa Flour 488 IgG (Invitrogen) as secondary antibodies. Nuclei were stained with Hoechst 33258 (1μg/mL). Autophagic vesicles formation was also confirmed after labelling with Enzo Autophagy kit reagents (MDC and Hoechst). Live cells were loaded with mitotracker red (Invitrogen) and fixed for co-localization analysis with activated Bax. Images were captured using Zeiss–Axiovert40 CFL microscope and processed using Image J software (NIH, USA).

Flow cytometery for Apoptosis Inducing Factor (AIF)

AIF antibody analysis was performed on flow cytometery using anti AIF FITC antibody and isotype control antibody from Santa Cruz Biotechnology, Santa Cruz, CA. Analysis was performed on BD FACSAria II at 488 nm excitation and 530 nm emission wavelengths.

Results are presented as fold increase in mean fluorescence intensity values with respect to control.

Lysotracker red uptake assay

Autophagy was assessed through monitoring lysotracker red (Invitrogen) uptake (normalized to cell tracker green in CeO_2 NPs-treated cells using previously described method. [45] The cells were analyzed at 530/590 nm excitation/emission for Lysotracker Red and 485/520 nm for Cell Tracker Green using a Biotech Powerwave XS plate reader.

Statistical Analysis

Every experiment was repeated using cells from 3–5 human subjects. Data are presented as average ± SD. Each experimental condition was done in triplicate for each individual. Data are analyzed by analysis of variance (ANOVA) followed by Bonferroni test for multiple comparisons using Graphpad software (Graphpad Prism 4.01, Graphpad Software Inc, San Diego, USA). A level of $p < 0.05$ (two-tailed) was considered significant.

Supplementary Material

Refer to Web version on PubMed Central for supplementary material.

Acknowledgments

References

1. Yu JC, Zhang L, Lin J. Direct Sonochemical Preparation of High-Surface-Area Nanoporous Ceria and Ceria-Zirconia Solid Solutions. J Colloid Interface Sci. 2003; 260:240–243. [PubMed: 12742056]

2. Khan SB, Faisal M, Rahman MM, Jamal A. Exploration of Ceo Nanoparticles as a Chemi-Sensor and Photo-Catalyst for Environmental Applications. Sci Total Environ. 2011; 409:2987–2992. [PubMed: 21570707]

3. Izu N, Shin W, Matsubara I, Murayama N. Development of Resistive Oxygen Sensors Based on Cerium Oxide Thick Film. Journal of Electroceramics. 2004; 13:703–706.

4. Corma A, Atienzar P, Garcia H, Chane-Ching JY. Hierarchically Mesostructured Doped Ceo2 with Potential for Solar-Cell Use. Nat Mater. 2004; 3:394–397. [PubMed: 15146175]

5. Kosynkin VD, Arzgatkina AA, Ivanov EN, Chtoutsa MG, Grabko AI, Kardapolov AV, Sysina NA. The Study of Process Production of Polishing Powder Based on Cerium Dioxide. Journal of Alloys and Compounds. 2000; 303:421–425.

6. Korsvik C, Patil S, Seal S, Self WT. Superoxide Dismutase Mimetic Properties Exhibited by Vacancy Engineered Ceria Nanoparticles. Chem Commun (Camb). 2007:1056–1058. [PubMed: 17325804]

7. Das M, Patil S, Bhargava N, Kang JF, Riedel LM, Seal S, Hickman JJ. Auto-Catalytic Ceria Nanoparticles Offer Neuroprotection to Adult Rat Spinal Cord Neurons. Biomaterials. 2007; 28 : 1918–1925. [PubMed: 17222903]

8. Tarnuzzer RW, Colon J, Patil S, Seal S. Vacancy Engineered Ceria Nanostructures for Protection from Radiation-Induced Cellular Damage. Nano Lett. 2005; 5:2573–2577. [PubMed: 16351218]

9. Chen J, Patil S, Seal S, McGinnis JF. Rare Earth Nanoparticles Prevent Retinal Degeneration Induced by Intracellular Peroxides. Nat Nanotechnol. 2006; 1:142–150. [PubMed: 18654167]

10. Rzigalinski BA, Meehan K, Davis RM, Xu Y, Miles WC, Cohen CA. Radical Nanomedicine. Nanomedicine (Lond). 2006; 1:399–412. [PubMed: 17716143]

11. Park B, Donaldson K, Duffin R, Tran L, Kelly F, Mudway I, Morin JP, Guest R, Jenkinson P, Samaras Z, et al. Hazard and Risk Assessment of a Nanoparticulate Cerium Oxide-Based Diesel Fuel Additive - a Case Study. Inhal Toxicol. 2008; 20:547–566. [PubMed: 18444008]

12. Health Effects Institute, (HEI). Evaluation of Human Health Risk from Cerium Added to Diesel Fuel. Communication. 2001; 9

13. Cassee FR, van Balen EC, Singh C, Green D, Muijser H, Weinstein J, Dreher K. Exposure, Health and Ecological Effects Review of Engineered Nanoscale Cerium and Cerium Oxide Associated with Its Use as a Fuel Additive. Crit Rev Toxicol. 2011; 41:213–229. [PubMed: 21244219]

14. Organisation for Economic Co-operation and Development, (OECD). List of Manufactured Nanomaterials and List of End Points for Phase One of the Oecd Testing Programme. 2008.

15. Ma JY, Zhao H, Mercer RR, Barger M, Rao M, Meighan T, Schwegler-Berry D, Castranova V, Ma JK. Cerium Oxide Nanoparticle-Induced Pulmonary Inflammation and Alveolar Macrophage Functional Change in Rats. Nanotoxicology. 2011; 5:312–325. [PubMed: 20925443]

16. Park EJ, Choi J, Park YK, Park K. Oxidative Stress Induced by Cerium Oxide Nanoparticles in Cultured Beas-2b Cells. Toxicology. 2008; 245:90–100. [PubMed: 18243471]

17. Cho WS, Duffin R, Poland CA, Howie SE, MacNee W, Bradley M, Megson IL, Donaldson K. Metal Oxide Nanoparticles Induce Unique Inflammatory Footprints in the Lung: Important Implications for Nanoparticle Testing. Environ Health Perspect. 2010; 118:1699–1706. [PubMed: 20729176]

18. Hirst SM, Karakoti AS, Tyler RD, Sriranganathan N, Seal S, Reilly CM. Anti-Inflammatory Properties of Cerium Oxide Nanoparticles. Small. 2009; 5:2848–2856. [PubMed: 19802857]

19. Xia T, Kovochich M, Liong M, Madler L, Gilbert B, Shi H, Yeh JI, Zink JI, Nel AE. Comparison of the Mechanism of Toxicity of Zinc Oxide and Cerium Oxide Nanoparticles Based on Dissolution and Oxidative Stress Properties. ACS Nano. 2008; 2:2121–2134. [PubMed: 19206459]

20. Lowe SW, Lin AW. Apoptosis in Cancer. Carcinogenesis. 2000; 21:485–495. [PubMed: 10688869]

21. Mattson MP. Apoptosis in Neurodegenerative Disorders. Nat Rev Mol Cell Biol. 2000; 1:120–129. [PubMed: 11253364]

22. Adrie C, Bachelet M, Vayssier-Taussat M, Russo-Marie F, Bouchaert I, Adib-Conquy M, Cavaillon JM, Pinsky MR, Dhainaut JF, Polla BS. Mitochondrial Membrane Potential and Apoptosis Peripheral Blood Monocytes in Severe Human Sepsis. Am J Respir Crit Care Med. 2001; 164:389–395. [PubMed: 11500338]

23. Li C, Liu H, Sun Y, Wang H, Guo F, Rao S, Deng J, Zhang Y, Miao Y, Guo C, et al. Pamam Nanoparticles Promote Acute Lung Injury by Inducing Autophagic Cell Death through the Akt-Tsc2-Mtor Signaling Pathway. J Mol Cell Biol. 2009; 1:37–45. [PubMed: 19516051]

24. Zhang Q, Yang W, Man N, Zheng F, Shen Y, Sun K, Li Y, Wen LP. Autophagy-Mediated Chemosensitization in Cancer Cells by Fullerene C60 Nanocrystal. Autophagy. 2009; 5:1107–1117. [PubMed: 19786831]

25. Stern ST, Zolnik BS, McLeland CB, Clogston J, Zheng J, McNeil SE. Induction of Autophagy in Porcine Kidney Cells by Quantum Dots: A Common Cellular Response to Nanomaterials? Toxicol Sci. 2008; 106:140–152. [PubMed: 18632727]

26. Man N, Yu L, Yu SH, Wen LP. Rare Earth Oxide Nanocrystals as a New Class of Autophagy Inducers. Autophagy. 2010; 6:310–311. [PubMed: 20104026]

27. Maiuri MC, Galluzzi L, Morselli E, Kepp O, Malik SA, Kroemer G. Autophagy Regulation by P53. Curr Opin Cell Biol. 2010; 22:181–185. [PubMed: 20044243]

28. Tasdemir E, Chiara Maiuri M, Morselli E, Criollo A, D'Amelio M, Djavaheri-Mergny M, Cecconi F, Tavernarakis N, Kroemer G. A Dual Role of P53 in the Control of Autophagy. Autophagy. 2008; 4:810–814. [PubMed: 18604159]

29. Sanfins E, Dairou J, Hussain S, Busi F, Chaffotte AF, Rodrigues-Lima F, Dupret JM. Carbon Black Nanoparticles Impair Acetylation of Aromatic Amine Carcinogens through Inactivation of Arylamine N-Acetyltransferase Enzymes. ACS Nano. 2011; 5:4504–4511. [PubMed: 21526848]

30. Zhang B, Xing Y, Li Z, Zhou H, Mu Q, Yan B. Functionalized Carbon Nanotubes Specifically Bind to Alpha-Chymotrypsin's Catalytic Site and Regulate Its Enzymatic Function. Nano Lett. 2009; 9:2280–2284. [PubMed: 19408924]

31. Gozuacik D, Kimchi A. Autophagy as a Cell Death and Tumor Suppressor Mechanism. Oncogene. 2004; 23:2891–2906. [PubMed: 15077152]

32. Gomes LC, Scorrano L. Mitochondrial Elongation During Autophagy: A Stereotypical Response to Survive in Difficult Times. Autophagy. 2011; 7:1251–1253. [PubMed: 21743300]

33. Green DR, Reed JC. Mitochondria and Apoptosis. Science. 1998; 281:1309–1312. [PubMed: 9721092]

34. Cande C, Cecconi F, Dessen P, Kroemer G. Apoptosis-Inducing Factor (Aif): Key to the Conserved Caspase-Independent Pathways of Cell Death? J Cell Sci. 2002; 115:4727–4734. [PubMed: 12432061]

35. Samuelsen M, Cecilie Nygaard U, Lovik M. Particles from Wood Smoke and Road Traffic Differently Affect the Innate Immune System of the Lung. Inhal Toxicol. 2009; 21:943–951. [PubMed: 19552530]

36. Lucarelli M, Gatti AM, Savarino G, Quattroni P, Martinelli L, Monari E, Boraschi D. Innate Defence Functions of Macrophages Can Be Biased by Nano-Sized Ceramic and Metallic Particles. Eur Cytokine Netw. 2004; 15:339–346. [PubMed: 15627643]

37. Hollingsworth JW, Maruoka S, Li Z, Potts EN, Brass DM, Garantziotis S, Fong A, Foster WM, Schwartz DA. Ambient Ozone Primes Pulmonary Innate Immunity in Mice. J Immunol. 2007; 179:4367–4375. [PubMed: 17878331]

38. Ireland JM, Unanue ER. Autophagy in Antigen-Presenting Cells Results in Presentation of Citrullinated Peptides to Cd4 T Cells. J Exp Med. 2011; 208:2625–2632. [PubMed: 22162830]

39. Celardo I, De Nicola M, Mandoli C, Pedersen JZ, Traversa E, Ghibelli L. Ce(3)+ Ions Determine Redox-Dependent Anti-Apoptotic Effect of Cerium Oxide Nanoparticles. ACS Nano. 2011; 5:4537–4549. [PubMed: 21612305]

40. Gojova A, Lee JT, Jung HS, Guo B, Barakat AI, Kennedy IM. Effect of Cerium Oxide Nanoparticles on Inflammation in Vascular Endothelial Cells. Inhal Toxicol. 2009; 21(Suppl 1): 123–130. [PubMed: 19558244]

41. Pairon JC, Roos F, Iwatsubo Y, Janson X, Billon-Galland MA, Bignon J, Brochard P. Lung Retention of Cerium in Humans. Occup Environ Med. 1994; 51:195–199. [PubMed: 8130849]

42. Hussain S, Boland S, Baeza-Squiban A, Hamel R, Thomassen LC, Martens JA, Billon-Galland MA, Fleury-Feith J, Moisan F, Pairon JC, et al. Oxidative Stress and Proinflammatory Effects of Carbon Black and Titanium Dioxide Nanoparticles: Role of Particle Surface Area and Internalized Amount. Toxicology. 2009; 260:142–149. [PubMed: 19464580]

43. Smiley ST, Reers M, Mottola-Hartshorn C, Lin M, Chen A, Smith TW, Steele GD Jr, Chen LB. Intracellular Heterogeneity in Mitochondrial Membrane Potentials Revealed by a J-Aggregate-Forming Lipophilic Cation Jc-1. Proc Natl Acad Sci U S A. 1991; 88:3671–3675. [PubMed: 2023917]

44. Hussain S, Thomassen LC, Ferecatu I, Borot MC, Andreau K, Martens JA, Fleury J, Baeza-Squiban A, Marano F, Boland S. Carbon Black and Titanium Dioxide Nanoparticles Elicit Distinct Apoptotic Pathways in Bronchial Epithelial Cells. Part Fibre Toxicol. 2010; 7:10. [PubMed: 20398356]

45. Neun BW, Stern ST. Monitoring Lysosomal Activity in Nanoparticle-Treated Cells. Methods Mol Biol. 2011; 697:207–212. [PubMed: 21116970]
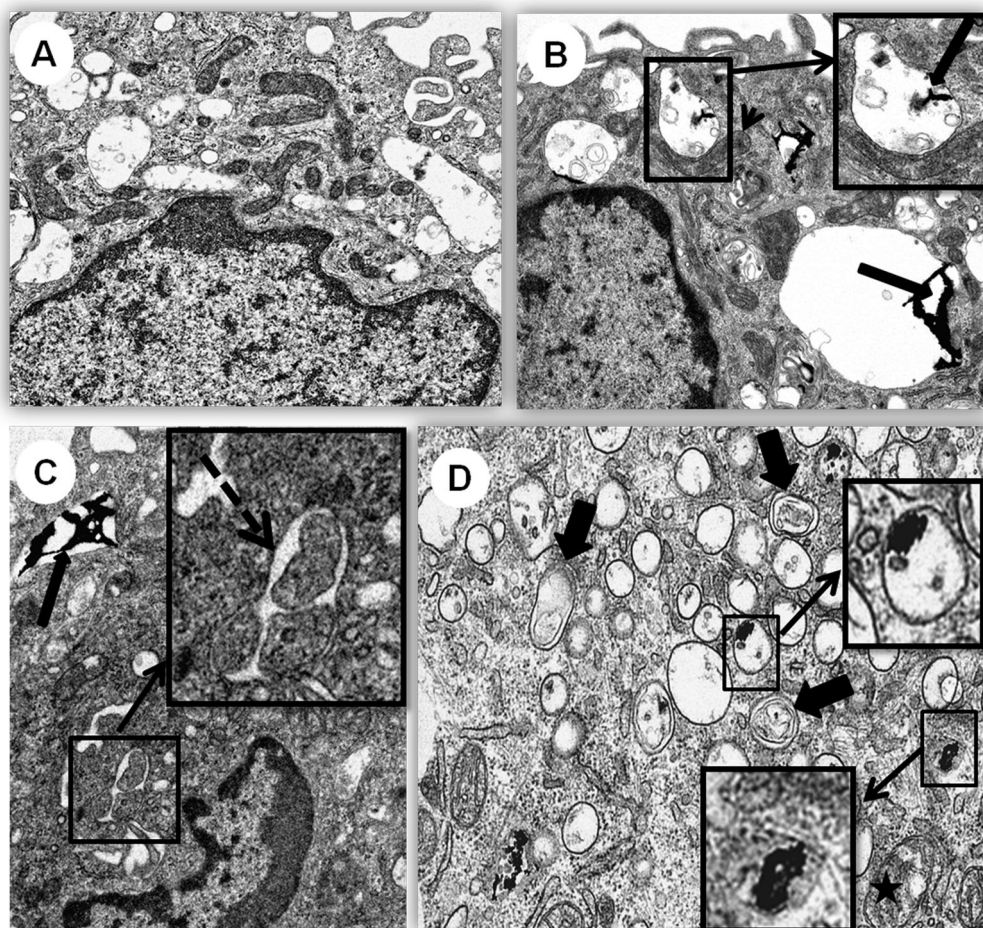
Figure 1.
TEM analysis of human monocytes after CeO_2 NP exposure. Cells were treated with 10 µg/mL CeO_2 NPs for 40 hours before analysis. Photo micrographs of A) Control, B), C) and D) CeO2 NP treated cells. Intracellular accumulation of CeO_2 NPs in vesicles (long arrows), enlargement of mitochondria (arrow head), autophagic vesicle formation (broken arrow), autolysosomes (thick short arrows), swollen mitochondria (asterisk). Insets presenting detailed structure of vesicle containing aggregate of CeO2 NPs (Figure1B), autophagic vesicle (Figure 1C) and ceria NPs inside vesicles and free in cytoplasm (Figure 1D). A, B and C 9900X, D 20500X.
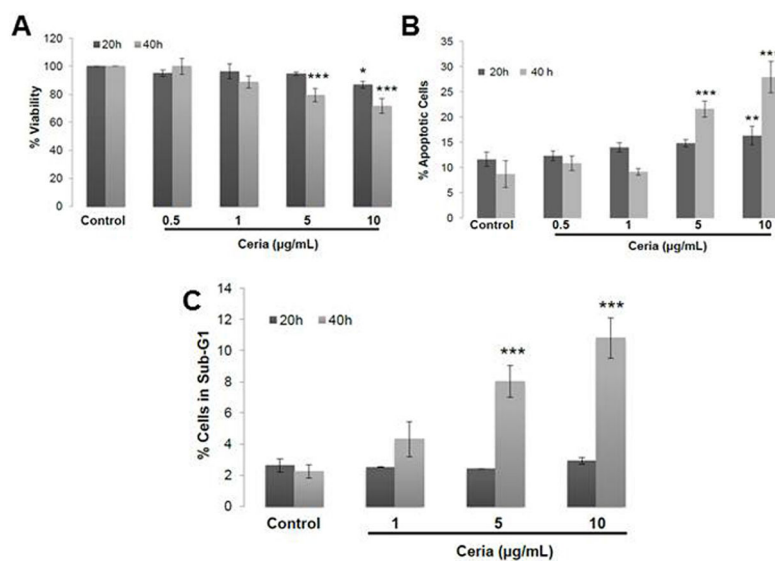
Figure 2.
Cell death detection after CeO_2 NP exposure. Cells were treated with different doses (0.5–10 µg/mL) of CeO_2 NPs for either 20 or 40 hours and analyzed for A) Cell viability by Calcein-AM staining and analyzed by spectrofluorimetry. B) Cell death (apoptosis *vs* necrosis) detection by staining with annexin/PI and analyzed by flow cytometery. Results are presented as % apoptotic cells (early+late apoptotic cells). More than 90% of the cells were Annexin positive and PI negative (A+/PI−). C) DNA fragmentation by measuring the Sub-G1 peak through flow cytometery. Data was analyzed by analysis of variance (ANOVA) followed by Bonferroni post hoc test. Graphs show average± SD, n= 3–5. *p<0.05, ** p<0.01 and *** p<0.001.
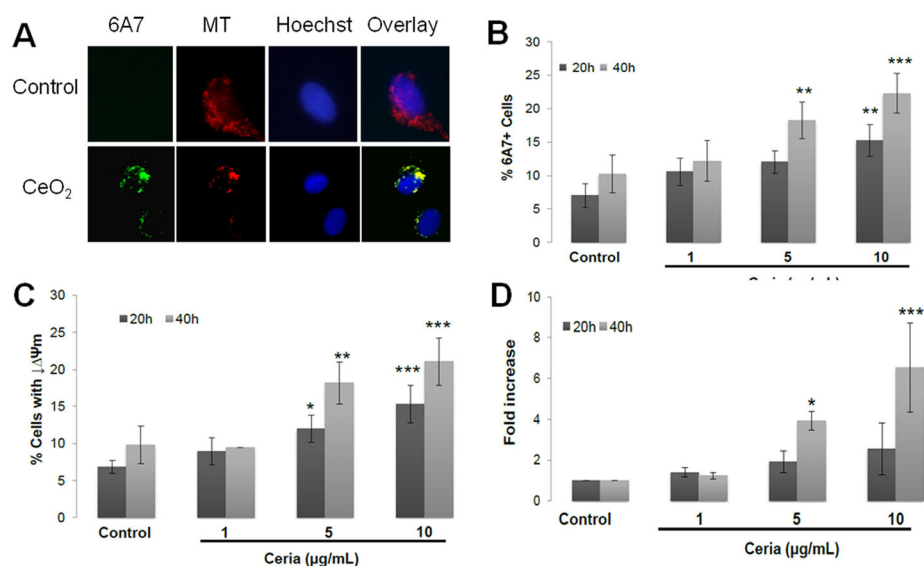
Figure 3.

Mitochondrial alterations after CeO_2 NP exposure. Cells were treated with different doses (1–10 μg/mL) of CeO_2 NPs for either 20 or 40 hours and analyzed for A) activation and mitochondrial relocation of pro-apoptotic protein Bax. Immunofluorescent images of cells showing activated form of bax relocating to mitochondria (co-localized with mitotracker red (MT) labelled mitochondria). B) Percent of 6A7 positive cells. At least 600 stained cells from each individual were counted to determine the percent of 6A7 positive cells. C) Loss of mitochondrial membrane potential (ψ_m) after staining with JC-1 probe. Cells were analyzed through flow cytometery. D) Apoptosis AIF protein expression using flow cytometery. Cells were stained with specific antibody for AIF and analyzed through flow cytometery. Results are presented as fold increase with respect to control (calculated using mean fluorescence intensity of the populations). Data was analyzed by analysis of variance (ANOVA) followed by Bonferroni post hoc test. Graphs show average± SD, n= 3–5. *p<0.05, ** p<0.01 and *** p<0.001.
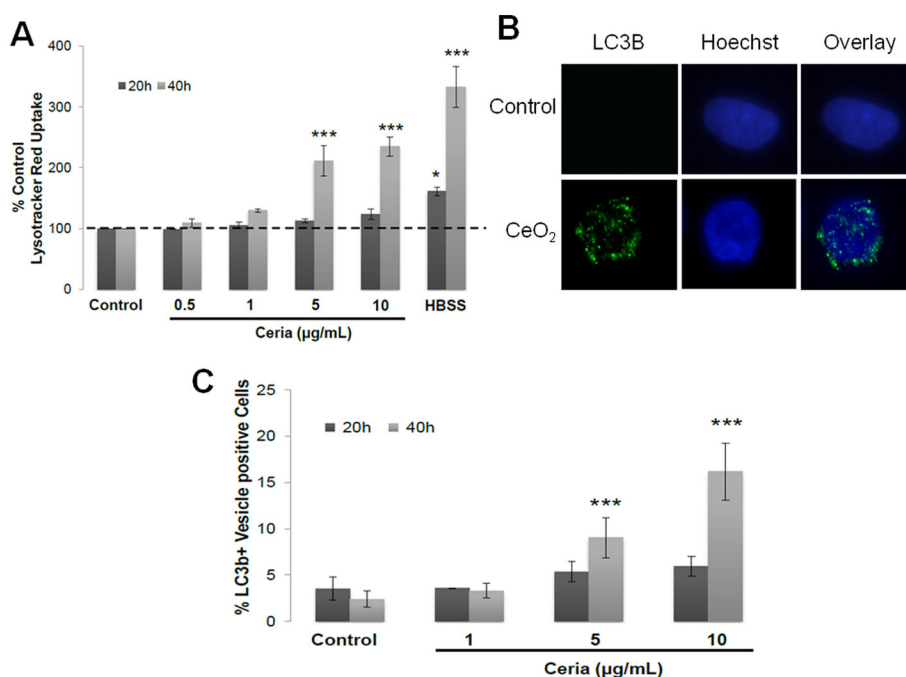
Figure 4.

Autophagy detection in CeO_2 NPs treated cells. Cells were treated with increasing doses (1–10 μg/mL) of CeO_2 NPs for 20 or 40 hours and analyzed for A) lysotracker red uptake assay. Cells were incubated with 50nM Lysotracker red and 10μM cell tracker green and analysis was performed through spectrofluorimetry. Results are presented as % Lysotracker red uptake with respect to control. HBSS treated cells were used as positive control for autophagy. B) Immunofluorescent images of cells showing LC3b protein marked vesicles through immunocytochemistry. C) Percent of LC3b+ vesicle containing cells. .At least 600 stained cells from each individual were counted to determine the LC3b positive cells. Data was analyzed by analysis of variance (ANOVA) followed by Bonferroni post hoc test. Graphs show average ± SD, n= 3–5. *$p<0.05$, ** $p<0.01$ and *** $p<0.001$.

Figure 5.
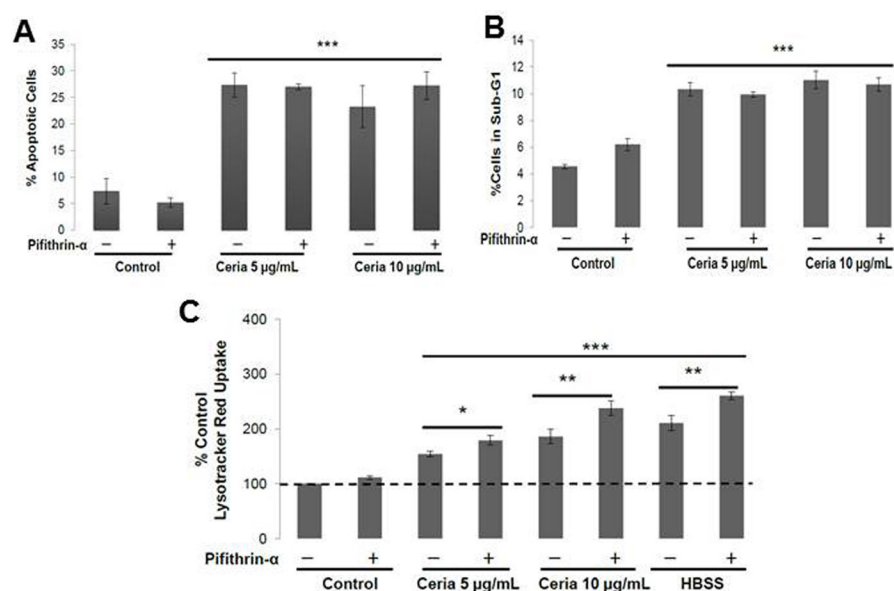Role of p53 in CeO_2 NP induced cell death. Cells were pre-incubated with pifithrin-α for 2 hours, treated with CeO_2 NPs (5 or 10 μg/mL) for 20 or 40 hours in its presence and analyzed through flow cytometery for A) Apoptosis detection by Annexin-V/PI staining B) Apoptosis detection through SubG-1 peak estimation C) Lysotracker red uptake assay. Data was analyzed by analysis of variance (ANOVA) followed by Bonferroni post hoc test. Graphs show average ± SD, n= 3–5. *p<0.05, ** p<0.01 and *** p<0.001.
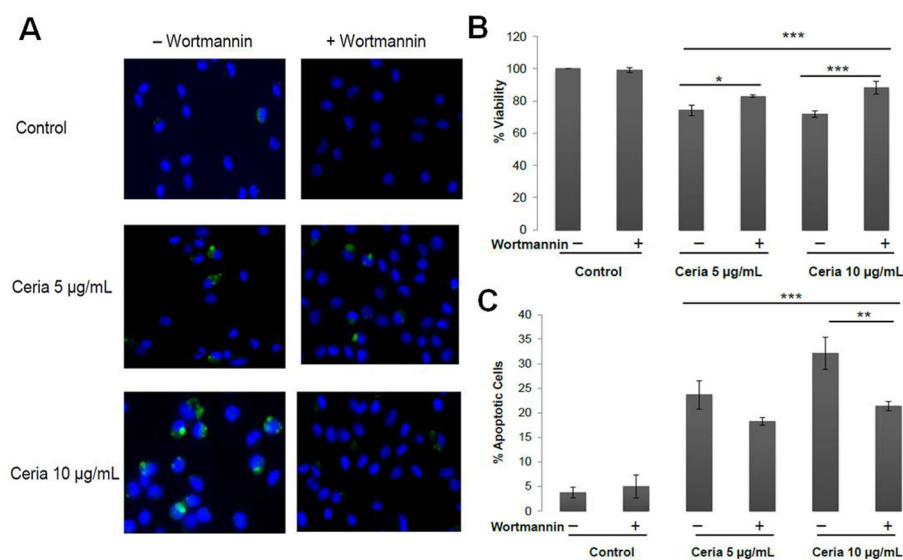
Figure 6.
Crosstalk between the autophagy and apoptosis induced by CeO_2 NPs. Cells were pre-incubated with autophagy inhibitor wortmannin (50nM) for 2 hours and then treated with CeO_2 NPs (5 or 10 μg/mL) for 20 or 40 hours in its presence and analyzed for A) Autophagic vesicle formations by MDC staining, nuclei were counterstained with Hoechst B) Cell viability by Calcein-AM staining C) Apoptosis detection by Annexin-V/PI staining. Data was analyzed by analysis of variance (ANOVA) followed by Bonferroni post hoc test. Graphs show average ± SD, n= 3–5 with triplicate of each condition each time. *p<0.05, ** p<0.01 and *** p<0.001.
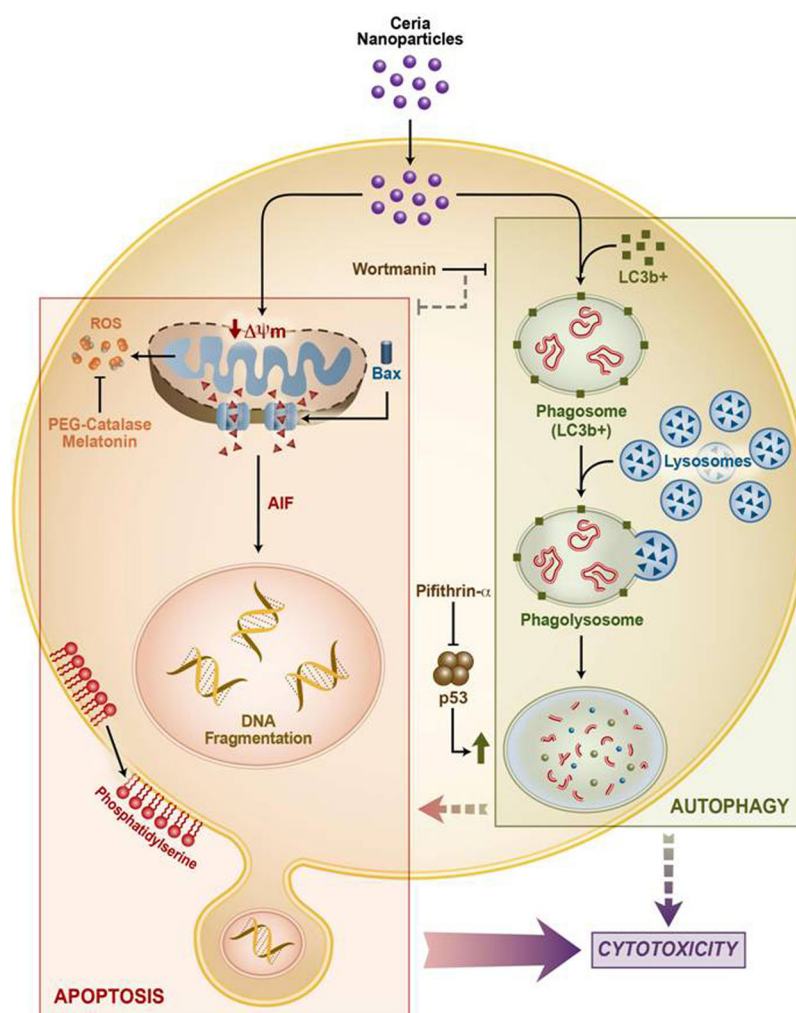
Figure 7.
Overview of the CeO_2 NP induced cell death pathways. CeO_2 NPs induce apoptosis through mitochondrial pathway (involving, activation and mitochondrial localization of Bax, $\downarrow \psi_m$ and over expression of AIF). CeO_2 NPs induced autophagy increased production of LC3b+ phagolysosomes. Inhibition of p53 by pifithrin-α increases the autophagy. Inhibition of autophagy through wortmannin decreases the cytotoxicity indicating pro-death role of autophagy.

Author Manuscript

Author Manuscript

Author Manuscript

Author Manuscript

Table 1

Characteristics of CeO$_2$ NPs

Primary Size		Hydrodynamic Diameter		Phase and Structure (XRD)	Surface Area (BET) m^2 g^{-1}	pH$_{iep}$ *	Morphology (TEM)	Zeta Potential mV		pDi**	EPM*** m^2 V^{-1} s^{-1}
TEM/SEM nm	XRD nm	EX-Vivo nm	Water nm					EX-Vivo (pH7.0) mV	Water (pH6.1) mV		
10–30	7	194(30)	231(16)	100% Cubic Ceria	93.8	7.8	irregular	−15(3)	19.1(6)	0.45	1.49±0.48 10^{-8}

*
Isoelectric point,

**
polydispersity Index,

***
Electrophoretic Mobility (in water)